Key Points:
- Nutrient inputs from land are fueling autochthonous DOM and POM production in coastal environment
- Organic matter characterization revealed its rapid transformation in the heterotrophic spiral
- Accumulated organic matter was characterized by small molecular size and high protein-like fluorescence

Correspondence to:
E. Asmala,
eero.asmala@helsinki.fi

Eutrophication Leads to Accumulation of Recalcitrant Autochthonous Organic Matter in Coastal Environment

Eero Asmala[1,2] (iD), Lumi Haraguchi[2] (iD), Stiig Markager[2] (iD), Philippe Massicotte[3] (iD), Bo Riemann[2] (iD), Peter A. Staehr[2] (iD), and Jacob Carstensen[2] (iD)

[1]Tvärminne Zoological Station, University of Helsinki, Hanko, Finland, [2]Department of Bioscience, Aarhus University, Roskilde, Denmark, [3]Takuvik Joint International Laboratory, Université Laval and Centre National de la Recherche Scientifique, Québec, Quebec, Canada

Abstract Anthropogenic nutrient enrichment is changing the structure and the function of coastal ecosystems. These coastal zones are transitions between freshwater and marine systems where multiple biogeochemical processes remove, produce, and transform organic matter. The extent to which the coastal zone is merely a conduit for terrestrial (allochthonous) organic matter versus a distinct source of autochthonous organic matter fueled by eutrophication is unclear. To address this issue, we characterized the freshwater and marine dissolved organic matter (DOM) pools in a eutrophic estuary with a long water residence time (Roskilde Fjord, Denmark) over an annual cycle. We combined elemental, optical (absorbance and fluorescence), and isotopic analyses to obtain insight about the bulk properties of the DOM pool during this period. We also used sediment traps to analyze the changes related to the exchange of organic matter between the particulate organic matter and DOM fractions. The results showed that labile autochthonous DOM from in situ primary production was rapidly transformed to more recalcitrant DOM that accumulated in the estuary despite continuous exchange with the open sea. Also, parts of the particulate organic matter pool were degraded rapidly (within 24 hr) and transformed into the DOM pool. Accumulated DOM was characterized by relatively low molecular size and stable carbon isotopic value and by high protein-like fluorescence. These results indicate that autotrophic material can be a major source of specific recalcitrant DOM in eutrophic coastal waters, contributing significantly to the flux of organic carbon to the ocean.

1. Introduction

The oceanic pool of organic carbon is about 660 Pg and is one of the largest dynamic carbon reservoirs on Earth, comparable to atmospheric CO_2 reservoir of ~750 Pg C (Jiao et al., 2010). Most of the organic carbon in seawater is in dissolved form and exceeds more than 200 times the amount of particulate carbon (Hansell et al., 2009). Rivers contribute with large terrestrial (allochthonous) dissolved organic matter (DOM) inputs (0.45 Pg C/year; Cole et al., 2007) through coastal environments to the oceanic carbon pool. Along with DOM, rivers transport nitrogen and phosphorus to the coastal systems, which have the potential of increasing primary production significantly (Cloern et al., 2014; Conley et al., 2009). This increase in primary production has led to widespread coastal eutrophication, which today is a global phenomenon affecting numerous ecosystems around the world (Boesch, 2002; Conley et al., 2002). The increased benthic and pelagic primary production is potentially a significant source of (autochthonous) DOM in coastal areas (Bertilsson & Jones, 2003; Myklestad, 1995; Staehr et al., 2018). In eutrophic coastal systems the autochthonous DOM production even exceeds the riverine load (Markager et al., 2011).

Autochthonous DOM is typically considered highly bioavailable and expected to be utilized rapidly in the microbial loop (Hopkinson et al., 1998; Søndergaard & Middelboe, 1995). However, estuaries with relatively small inputs of allochthonous carbon and high inputs of inorganic nutrients may act as *reactors* where autochthonous carbon dominates over the allochthonous (Markager et al., 2011). The characteristics and fate of autochthonous carbon in coastal systems is poorly known. In general, organic matter follows the so-called reactivity continuum, where the most bioavailable (labile) fractions of the pool are utilized first and the bioavailability of the whole pool gradually decreases (Amon & Benner, 1996; Hansell, 2013; Vähätalo et al., 2010). However, organic matter bioavailability is not determined solely by its inherent properties but also by the prevailing environmental conditions (Marín-Spiotta et al., 2014).

In estuarine and coastal systems, DOM and other constituents are affected by two different general mechanisms: mixing and processing (Asmala et al., 2016). Pure physical mixing of the two end-members (riverine and marine) results in predictable characteristics of the DOM pool relative to salinity as long as the end-member values are known (Officer, 1979). Biogeochemical processes include photomineralization, flocculation, heterotrophic consumption, and autochthonous production, all of which result in distinct alterations to the DOM pool (Asmala et al., 2014, 2018; Moran et al., 2000; Rochelle-Newall & Fisher, 2002). The net effects of the biogeochemical processes within the coastal system define whether the DOM pool follows apparent conservative mixing in estuaries or deviate from such a pattern. Even though that changes in the DOM pool along coastal salinity gradients have been studied comprehensively, a coherent view of the balance between mixing and processing (removal, production, and transformation) is missing. Some studies report conservative behavior of DOM along the salinity gradient (Abril et al., 2002; Bowers et al., 2004; Guo et al., 2007; Mantoura & Woodward, 1983; Spencer et al., 2007), whereas other studies show significant nonconservative dynamics in the DOM pool, indicating net removal or production within the coastal system (Asmala et al., 2014; Huguet et al., 2009; Markager et al., 2011; Uher et al., 2001). Specifically, production and fate of DOM in systems affected by eutrophication are poorly understood, despite that coastal eutrophication is a widespread phenomenon around the world (Cloern, 2001).

In this study, we addressed two major challenges in the use of the conservative mixing approach: inherent variability (e.g., seasonal patterns) in observations along the salinity gradient and relatively small changes due to short residence time in many coastal systems. First, as many nutrient or DOM constituents follow a seasonal pattern, it is necessary to capture this variation for a given system. To address this issue, we conducted a sampling campaign that covered an annual cycle. Second, as many estuarine and coastal system have short freshwater residence times, that is, the system is flushed on relatively short time scales (days to weeks), the extent of processing of nutrients and DOM within the system is short and challenging to quantify with most current analytical approaches. As our study area has relatively long residence time (up to 2 years in the inner estuary), the signal for autochthonous production and DOM diagenesis is expectedly stronger than in those systems with shorter residence times (Markager et al., 2011), thus allowing better quantification of the deviations from conservative mixing.

Our objective was to expand current views of coastal processing of DOM by unraveling the role of autochthonous DOM and its transformation within the system. We also characterized the coastal DOM pools with different analytical approaches to get a coherent view of the characteristics of DOM in a system dominated by autochthonous DOM inputs. We further aimed to identify the major biogeochemical DOM processing pathways for autochthonous DOM. We hypothesize that (1) DOM produced and processed within the coastal system will have a distinct fingerprint compared to stream or open sea sources and (2) biogeochemical processing of this autochthonous DOM will rapidly transform it into a more recalcitrant pool of DOM.

2. Material and Methods

2.1. Field Sampling and Location

Roskilde Fjord is a shallow, microtidal estuary with a narrow opening in the northern part to Kattegat, Baltic Sea (Figure 1). Mean depth is 4 m, but due to the relatively small catchment and resulting low river discharge, the freshwater residence time is high, up to 8 months for the inner (southern) part of the Roskilde Fjord (Kamp-Nielsen, 1992). Streams draining catchments dominated by agriculture are scattered along the estuarine coastline, resulting in high nutrient inputs to the coastal system, which has enhanced primary production and eutrophication (Pedersen et al., 2014; Riemann et al., 2016; Staehr et al., 2017). Despite the relatively high nutrient inputs to the estuary, the shallow depth and efficient mixing in the system keeps the water well oxygenated throughout the year (Staehr et al., 2017).

We sampled three estuarine and five stream stations in Roskilde Fjord on 22 occasions between May 2014 and November 2015 (Figure 1). There is a narrow channel-like connection between the inner (southern) and outer (northern) parts of Roskilde Fjord, limiting the water exchange between them. Our sampling strategy was designed to take this feature into account. The sampling was carried out in the two main parts of the estuary, its boundary with the Kattegat and the majority of the freshwater sources draining into the system. Stream samples were taken from the surface only, whereas marine water was sampled from two depths, 1
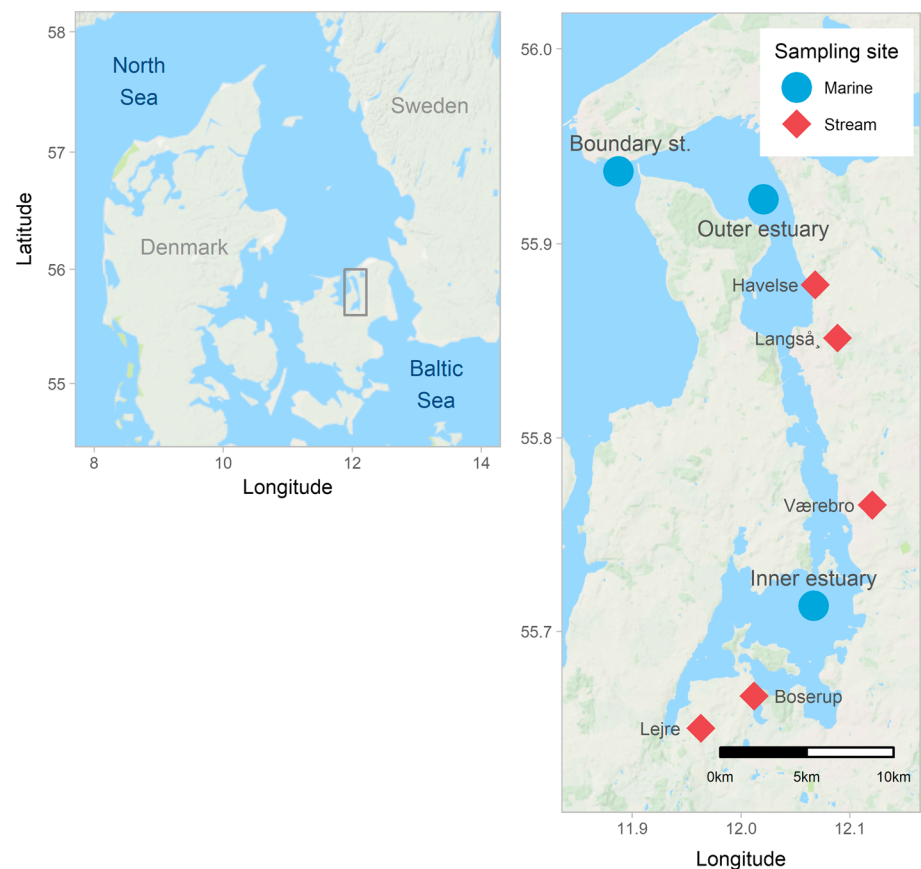
Figure 1. Map of the sampling locations.

and 4 m at each site. To investigate the exchange between the particulate and dissolved fractions of organic matter (POM and DOM, respectively), we deployed sediment traps in the inner and outer parts of the estuary on five occasions between March and November in 2015. The sediment traps consisted of four identical plexiglass cylinders with an inner diameter of 7.5 cm and height of 45 cm (aspect ratio of 6:1). Traps were deployed at 2-m depth for 24 hr. Effectively, sediment traps act as in situ experimental units for studying the short-term microbial transformations of organic matter from particulate to dissolved phase (Nagata et al., 2000). Deployments in both inner and outer parts enabled comparisons of biogeochemical processing of the settling material between systems with low and high residence time. After collection, samples from the water column and sediment traps were kept cold and in the dark before filtering in the laboratory within 6 hr after sampling. Samples were filtered with precombusted (4 hr at 450 °C) glass fiber filters (GF/F, Whatman, USA), and aliquots for subsequent analyses were taken. Samples for nutrients (nitrogen and phosphorus fractions), DOC, and size exclusion chromatography (SEC) were stored frozen until analysis. Samples for colored dissolved organic matter (CDOM) and DOM fluorescence (FDOM) were stored refrigerated until analysis.

2.2. Analytical Procedures

Total nitrogen (TN) and total phosphorus (TP) were measured from unfiltered water samples, and total dissolved nitrogen, total dissolved phosphorus, ammonium, nitrite, nitrate (dissolved inorganic nitrogen; DIN), and phosphate (dissolved inorganic phosphorus; DIP) were measured from filtered water samples. Nutrient analyses were carried out using the techniques described by Hansen and Koroleff (1999). Dissolved organic nitrogen (DON) and dissolved organic phosphorus (DOP) were inferred by subtracting DIN and DIP from total dissolved nitrogen and total dissolved phosphorus, respectively. DOC was measured with a Shimadzu TOC-V_{CPH} analyzer. The accuracy of measured DOC concentrations was controlled by analyzing a seawater

reference standard provided by the consensus reference material program. CDOM absorption was measured using a Shimadzu 2401PC spectrophotometer with 5-cm quartz cuvette over the spectral range from 200 to 800 nm at 1-nm intervals. Ultrapure water was used as the blank for all samples. Excitation-emission matrices (EEMs) of FDOM were measured with a Varian Cary Eclipse fluorometer (Agilent). A blank sample of ultrapure water was removed from EEMs, as well as the scattering bands. EEMs were corrected for inner filter effects with absorbance spectra (Murphy et al., 2010) and Raman calibrated by normalizing to the area under the Raman scatter peak (excitation wavelength of 350 nm) of an ultrapure water sample run on the same session as the samples. The molecular size of DOM was analyzed with SEC. The SEC analyzer consisted of a Shimadzu high-performance liquid chromatography system (Shimadzu Corporation, Kyoto, Japan) equipped with a linear-type column (TSK $G2000SW_{XL}$ column [7.8 × 300 mm, 5-μm particle size], Tosoh Bioscience GmbH), a guard column (Tosoh Bioscience GmbH), and a UV-Vis diode array (Shimadzu SPD-M10AVP) set to 250 nm. The eluent was 0.01 M acetate buffer at a pH of 7.00 (Vartiainen et al., 1987). The system was calibrated using acetone and polystyrene sulphonate (PSS) of 1, 3.5, 4.2,, 6.5, and 11 kDa (58, 1,100, 3,610, 4,230, 6,520, and 10,600 Da, respectively). Sample runs were calibrated daily. Log-linear calibration curve was used over the apparent molecular weight range tested. From corrected and integrated SEC chromatogram we calculated the number averaged apparent molecular weight (Chin et al., 1994). For stable carbon isotope analysis, frozen and acidified water samples were processed at the Stable Isotope Facility at UC Davis (USA). Samples were analyzed for $\delta^{13}C$ using a O.I. Analytical Model 1030 TOC Analyzer (Xylem Analytics, College Station, TX) interfaced to a PDZ Europa 20-20 isotope ratio mass spectrometer (Sercon Ltd., Cheshire, UK) utilizing a GD-100 Gas Trap Interface (Graden Instruments). The resulting carbon delta values are expressed relative to the international standard Vienna PeeDee Belemnite. Reported analytical precision for this method is ±0.4‰.

2.3. Statistical Analyses

For assessing the terrestrial signature and the initial quality of the DOM pool, fluorescence peaks (peaks A, C, M, and T; Coble, 1996), humification index (HIX; Zsolnay et al., 1999) and biological index (BIX; Huguet et al., 2009) were calculated from the measured and corrected EEMs. Processing of the EEMs was done using the eemR package for R software (Massicotte, 2018). In order to resolve the *fingerprints* of the different DOM sources (autochthonous vs. allochthonous), we used the parallel factor analysis (PARAFAC; Stedmon et al., 2003) to distinguish different components of the measured and corrected EEMs (Murphy et al., 2008). PARAFAC modeling was done following the protocol by Murphy et al. (2013). Successive models from four to nine components were fitted using the DrEEM Matlab toolbox. Based on split-half analysis, a model with nine components was found to adequately model the fluorescence variability over the samples ($R^2 = 0.999$). Component details are shown in supporting information Figure S1. The identified components were compared to previously validated components using the OpenFluor fluorescence database (http://www.openfluor.org/), and main characteristics are presented in Figure S1. PARAFAC components were used for *k*-means clustering analysis using the Hartigan-Wong algorithm (Hartigan & Wong, 1979) to identify groups of stations with similar DOM characteristics. A nonparametric modeling approach, generalized additive model (Hastie & Tibshirani, 1990), was used to test for the possible seasonality in nutrient and DOM observations. A generalized additive model was carried out with R software using the *mgcv* package (Wood, 2011). In summary, the number of smoothing terms was chosen by generalized cross-validation, and cyclic cubic regression splines were used for smoothing. To visualize the possible net production and consumption along the salinity gradient, we used a modification of the conservative mixing model approach (CMM; Officer, 1979). In this approach, two end-members along the salinity gradient are defined for each constituent separately, and the end-members are linearly connected. CMM approach is challenging when the scale of the variability of the end members is uncertain (Asmala et al., 2016). However, a straight line relationship between concentration and salinity can be expected in an estuary if stream discharge and constituent concentration in the stream vary but with a short time scale compared to the flushing time of the estuary (Bowers & Brett, 2008). This is the case in Roskilde Fjord, where the freshwater transit from inner estuary is up to 8 months on average (Kamp-Nielsen, 1992). In this study, we used simple linear regression to connect all observations from the two end-members defined by the *k*-means clustering analysis. Inner estuary was excluded from the regression to allow analysis of deviations from CMM. Positive deviations from the conservative mixing at the inner estuary station indicate net production, and negative deviations indicate net consumption of the constituent. Deviations from conservative mixing were quantified for observations from the
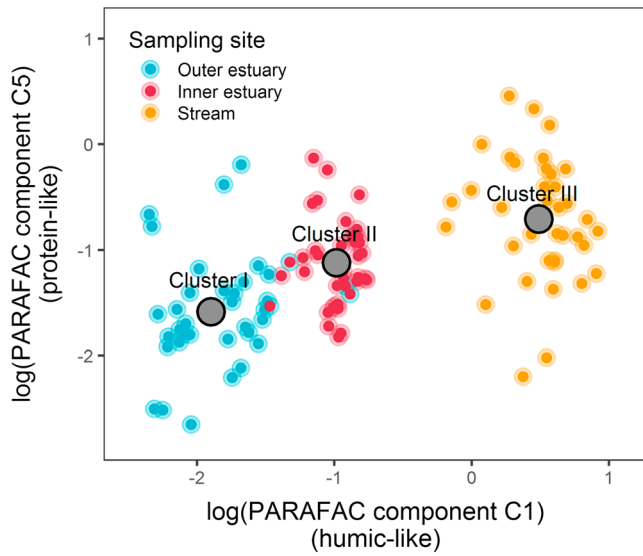
Figure 2. Log-transformed fmax values of PARAFAC components C1 (primary humic-like) and C5 (primary protein-like). The color of the outer circle indicates the actual sampling location, whereas the smaller circle shows the cluster assigned by the *k*-means clustering analysis. Points with different colors in the inner and outer circle are mismatches between the cluster assigned by the *k*-means analysis and true sampling location. Gray points show the location of the mean value of each *k*-mean cluster. PARAFAC = parallel factor analysis.

inner estuary for nutrient and DOM variables, expected (from the CMM) values were subtracted from observations, and the results were divided by the expected to quantify the relative difference. One-sample *t* test was used to test if group mean for each nutrient and DOM variable deviated significantly from CMM. If the test indicated significant deviation from CMM, the amount of deviation was used in further analysis. Although the *t* test did not account for the uncertainty of the CMM used for standardizing the variables, the effect of this was small because salinities in the inner estuary occupied the approximate midrange between the salinities of the two end-members where the confidence intervals of the CMM are narrow and substantially smaller than variations among observations of relative difference.

3. Results

3.1. DOM Properties

Salinity and temperature profiles at the marine stations showed that the water column was well mixed. We did not find any significant difference between surface and bottom samples for any of the study variables. Therefore, we considered surface and bottom samples from each marine sampling as replicates. Observations were divided into three distinctive groups: streams (five stations), inner estuary (one station), and outer estuary (two stations). This approach was validated using *k*-means clustering analysis for DOM variables, which yielded an accuracy of 96% in dividing the data in the three predefined clusters (Figure 2; 107 correct groupings of 111 observations). These three groups were used in the analyses of the DOM pathways in the system.

3.2. Seasonal Patterns in Nutrients and DOM

We sampled longer than an entire annual cycle, capturing the intra-annual variability of the estuary (Figure 3). DIN was lowest during late spring and early summer and highest during autumn–winter at the marine stations (Figure 3a). At stream stations, DIN concentrations were considerably higher, also with a significant decrease during summer and increasing during the nonproductive autumn and winter periods. DIP concentrations were relatively low and without any distinctive seasonal pattern in streams and outer estuary. The
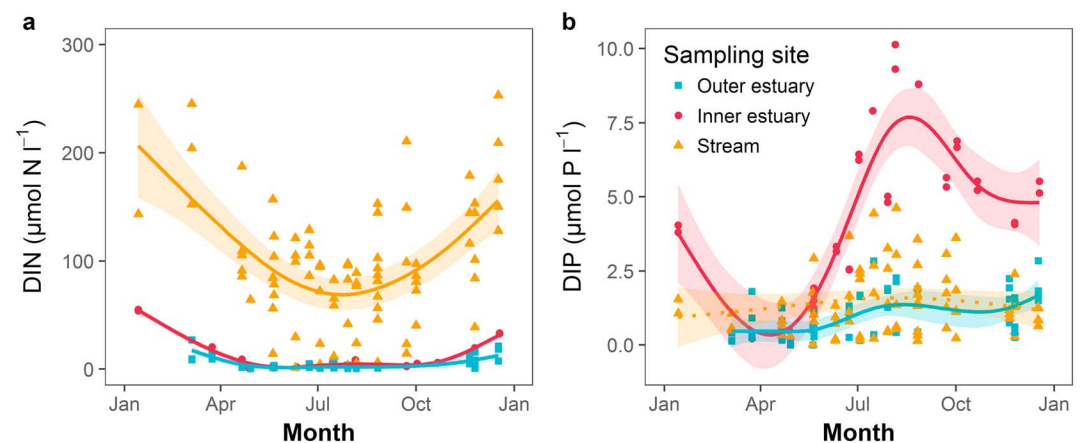

Figure 3. The observed concentrations of (a) DIN (NO_2^-, NO_3^-, and NH_3^+) and (b) DIP (PO_4^{3-}), and the estimated annual cycle from the GAM approach with 95% confidence interval marked by shaded area. Observations with significant ($p < 0.05$) temporal source of variation as revealed by the GAM analysis are marked with a solid line. A dotted line indicates no significant temporal variation. DIN = dissolved inorganic nitrogen; DIP = dissolved inorganic phosphorus; GAM = generalized additive model.
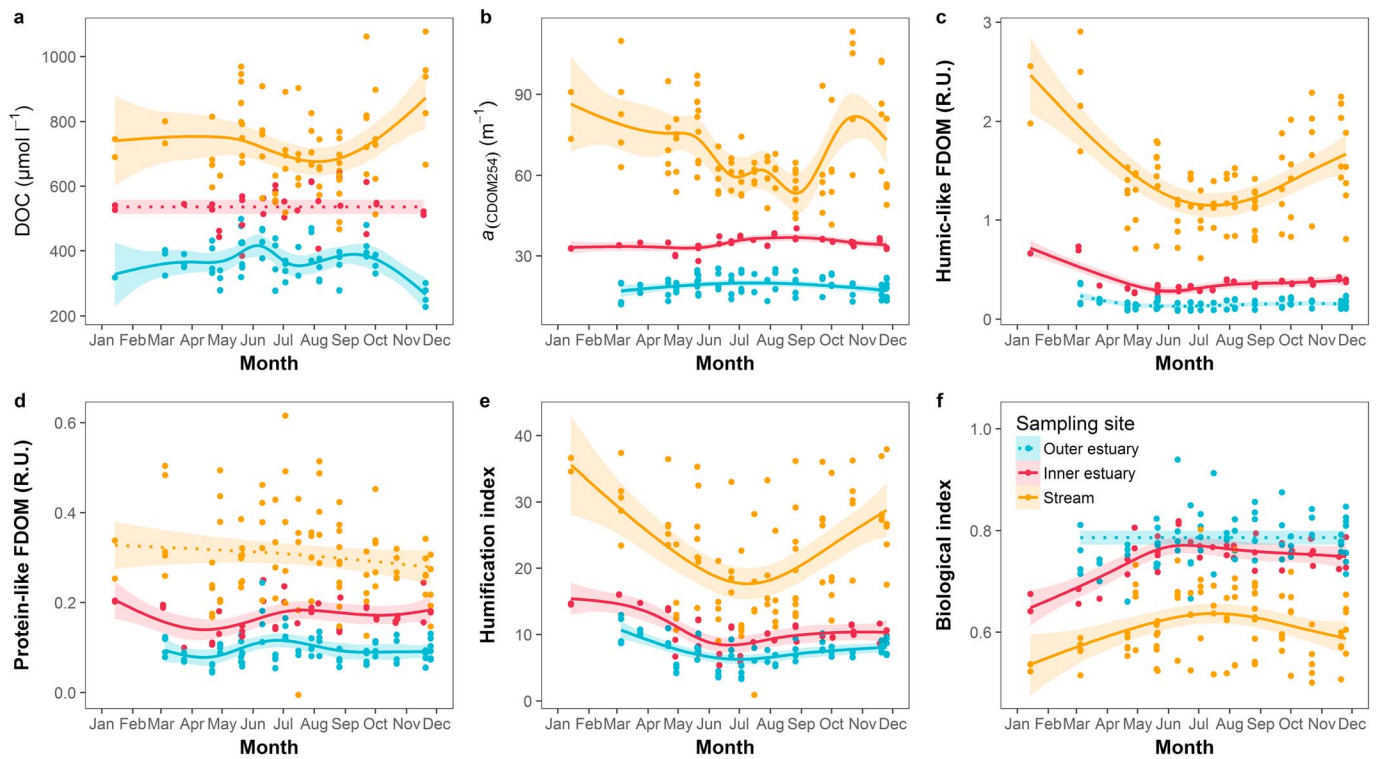
Figure 4. The observed DOM characteristics and the estimated annual cycle from the GAM approach with 95% confidence interval marked by shaded area. (a) Dissolved organic carbon, (b) CDOM absorption coefficient at 254 nm, (c) humic-like CDOM fluorescence (peak C), (d) protein-like CDOM fluorescence (peak T), (e) humification index (HIX), and (f) biological index (BIX). Observations with significant ($p < 0.05$) temporal source of variation as revealed by GAM are marked with a solid line. A dotted line indicates no temporal pattern. DOM = dissolved organic matter; GAM = generalized additive model; CDOM = colored dissolved organic matter; DOC = dissolved organic carbon; FDOM = DOM fluorescence.

inner estuary displayed a sharp increase in July–August indicating enhanced microbial remineralization and release from the sediment, resulting in high DIP levels sustained until the temperature decreases and oxygen penetrates deeper into sediments in autumn, followed again by nutrient uptake during the spring bloom (Figure 3b).

Seasonal patterns in DOM characteristics were in general more pronounced in the freshwater streams compared to the marine system (Figure 4 and Table S1). For DOC in marine samples, the annual maxima in concentration were reached in summer–autumn and minimum values during winter–spring (Figure 4a). In streams, the annual pattern was almost opposite, with the highest concentrations observed during winter and lowest during autumn. CDOM absorption at 254 nm ($a_{CDOM(254)}$) showed only weak seasonal pattern in marine stations, but in streams it corresponded to the dynamics of DOC (Figure 4b). Humic-like fluorescence (peak C; Figure 4c) and HIX (Figure 4e) showed similar patterns as $a_{CDOM(254)}$, apart from the increase at marine stations in early spring. Protein-like fluorescence (peak T) appeared to have two annual maxima: winter and summer (Figure 4d). BIX was overall higher in the marine system compared to the freshwater system and peaked during summer (Figure 4f). Seasonal patterns of PARAFAC components are shown in Figure S3. Overall, DOM quantity (as indicated by DOC concentration) and terrestrial characteristics (CDOM absorption and humic-like fluorescence as proxies) were higher in the streams compared to the marine sampling stations.

3.3. CMM Analysis

The CMM approach revealed large variation in the DOM variables at both end-members (Figure 5). The uncertainty introduced to CMM by this variation could be overcome by having enough observations covering more than an annual cycle. The CMM indicates production of DOC, $a_{CDOM(254)}$, and protein-like fluorescence (Figures 5a, 5b, and 5d) in the inner estuary. There was a decrease in humic-like fluorescence and molecular weight (Figures 5e and 5f), whereas $a_{CDOM(440)}$ showed both increased and decreased observations along the salinity gradient (Figure 5c).

AGU
100
ADVANCING EARTH
AND SPACE SCIENCE

Global Biogeochemical Cycles
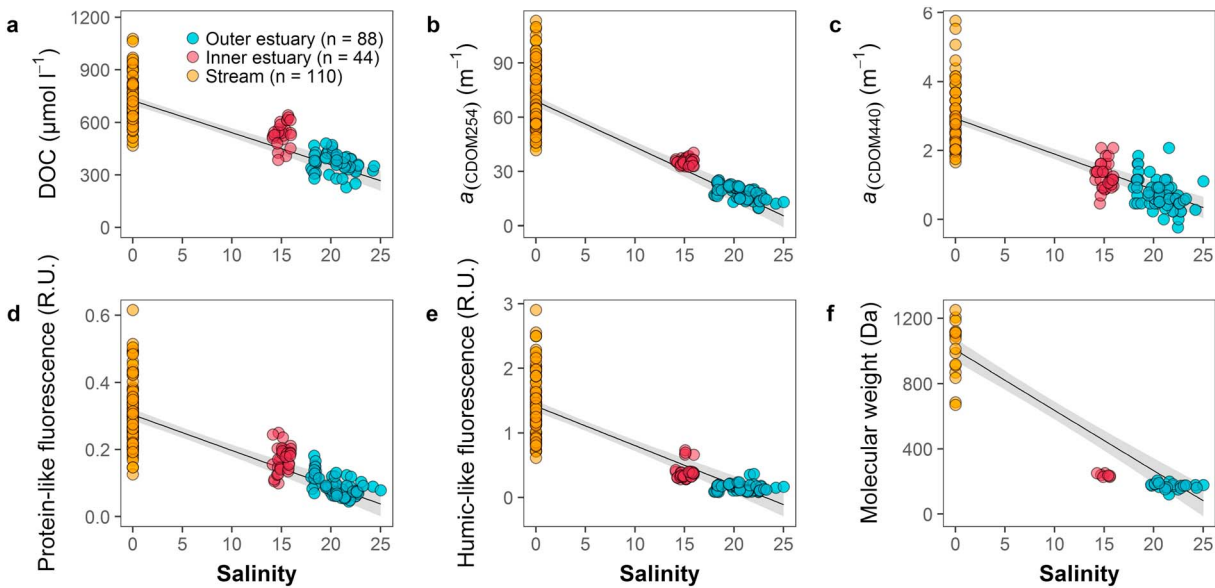
10.1029/2017GB005848

Figure 5. DOM variables along the estuarine salinity gradient in Roskilde Fjord; (a) dissolved organic carbon, (b) CDOM absorption coefficient at 254 nm, (c) CDOM absorption coefficient at 440 nm, (d) protein-like CDOM fluorescence (peak T), (e) humic-like CDOM fluorescence (peak C), and (f) DOM molecular weight. Conservative mixing line (black line) is drawn using linear regression between the observations of stream samples (yellow circles) and outer and boundary station samples (blue circles). Gray area indicates 95% confidence band around the slope of the regression line. Observations from the inner estuary (red circles) below the mixing line indicate net decrease in the respective variable, whereas observations above indicate net increase. DOM = dissolved organic matter; CDOM = colored dissolved organic matter; DOC = dissolved organic carbon.
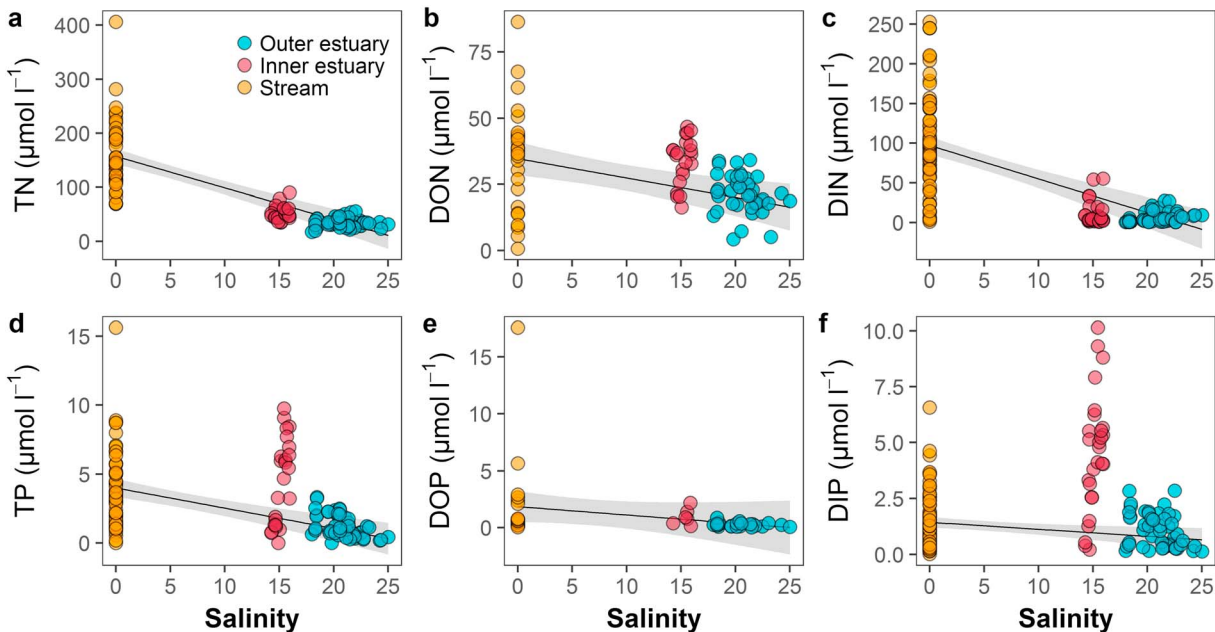

Figure 6. Nutrient concentrations along the estuarine salinity gradient in Roskilde Fjord. (a) TN = total nitrogen; (b) DON = dissolved organic nitrogen; (c) DIN = dissolved inorganic nitrogen; (d) TP = total phosphorus; (e) DOP = dissolved organic phosphorus; and (f) DIP = dissolved inorganic phosphorus. Conservative mixing line (black line) is drawn using linear regression between the observations of stream samples (yellow circles) and outer and boundary station samples (blue circles). Gray area indicates 95% confidence band around the slope of the regression line. Observations from the inner estuary (red circles) below the mixing line indicate net decrease, whereas observations above the mixing line indicate net increase.
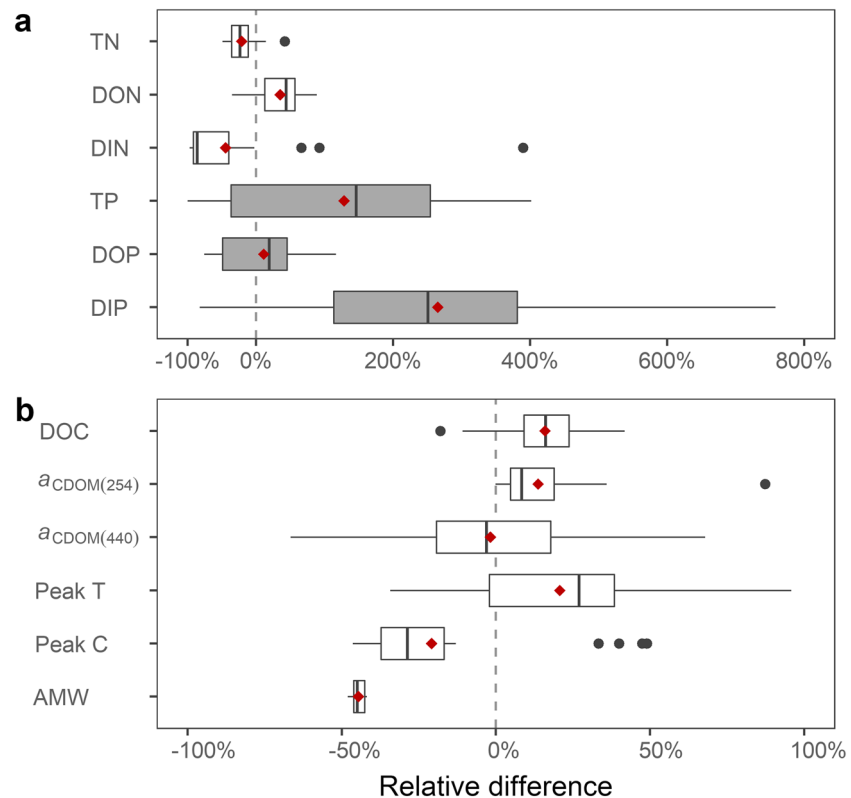
Figure 7. Relative differences between observed and predicted nutrient (a) and DOM variables (b) in the inner estuary. Predictions are based on a CMM. Relative deviations for phosphorus are marked in gray to separate them from nitrogen fractions. Lower and upper ends of boxes indicate the IQR (Q3–Q1) and whiskers the lowest and the highest values within the range of 1.5 IQR. Thick black line indicates median value, red diamond mean value of each group. Circles denote outliers in the data. Dashed vertical line at value 0 indicates no difference between observed and predicted value = conservative mixing. Negative values indicate lower observed values compared to predicted, whereas positive values indicate higher. All variables except DOP and $a_{CDOM(440)}$ deviated significantly ($p < 0.05$; Table S2) from CMM. DOM = dissolved organic matter; CMM = conservative mixing model approach; IQR = interquartile range; DOP = dissolved organic phosphorus.

We used the CMM approach for also nitrogen and phosphorus to examine the possibility of coupled processes between nutrients and DOM (Figure 6). Results indicate a significant production of DON, TP, and DIP in the inner estuary, whereas losses of total and inorganic nitrogen (TN and DIN) were observed there. DOP had high uncertainties due to limited number of observations and showed no apparent deviations from CMM.

In general, the 95% confidence interval was very close to the slope of the regression line for most variables (Figures 6 and 7). This results from the high number of observations and their relatively low variance around the mean value (Table S3 and Figures S5 and S6). There is large range between the minimum and maximum value for each parameter and group, but most observations are centered around the mean value. To quantify the deviations from the CMM at the inner estuary sampling station, we used the differences between the observed values and the values expected from the CMM. Deviations from conservative mixing was not significant for DOP and $a_{CDOM(440)}$, while for other variables in Figure 7 the deviations were significant (Table S2). In order to compare different DOM variables having different scales and units, relative differences between observed and expected values were used (Figure 7). On average, DOC concentrations in the inner estuary were 16% higher than the value expected from the CMM (Figure 7a). Production of $a_{CDOM(254)}$ and protein-like fluorescence were on the same level as DOC (14 and 21%, respectively). On the other hand, there was net consumption of humic-like fluorescence (−13%) and molecular weight (−45%). Quantification of the deviations revealed that DON concentrations were on average 35% higher than expected in the inner estuary, and TP and DIP were 129% and 265% higher, respectively (Figure 7). TN was 21% lower than expected, whereas DIN deviated on average −44%.
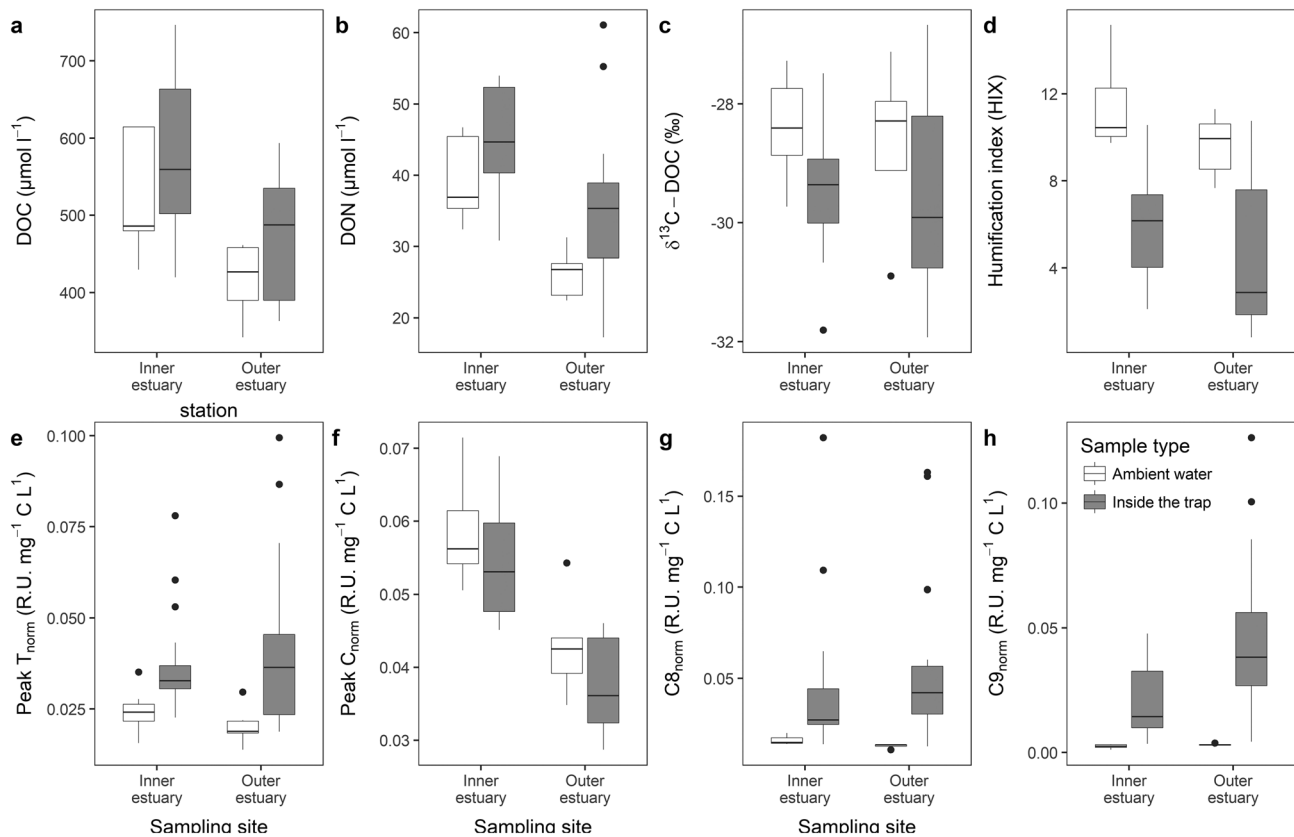
Figure 8. DOM characteristics inside the sediment traps after 24 hr deployment and outside the traps (ambient water column conditions). (a) Dissolved organic carbon, (b) dissolved organic nitrogen, (c) stable carbon isotope value of dissolved organic carbon, (d) humification index (HIX), (e) DOC-normalized protein-like fluorescence, (f) DOC-normalized humic-like fluorescence, (g) DOC-normalized fluorescence of PARAFAC component C8, and (h) DOC-normalized fluorescence of PARAFAC component C9. Lower and upper ends of boxes indicate the IQR (Q3–Q1) and whiskers the lowest and the highest values within the range of 1.5 IQR. Thick black line indicates median value. Circles denote outliers in the data. DOM = dissolved organic matter; IQR = interquartile range; DOC = dissolved organic carbon; DON = dissolved organic nitrogen.

3.4. Release of DOM From Sinking Particles

DOM characteristics from inside the sediment traps were compared with the ambient DOM just outside the traps (Figure 8). We considered the differences between the inside and outside (ambient) organic matter pools as resulting from both the exchange between POM and DOM fractions and biological processing of DOM. Settling POM contains both nonliving particles and phytoplankton cells, potentially producing fresh organic matter during the 24-hr incubations (Figure S4). There was a large variation in observed DOC, but on average, inside the sediment traps there was an increase of 62 and 53 μmol/L (inner and outer estuary, respectively) compared to the ambient water during the 24-hr deployments (Figure 8a). DON increased in the traps, with an average of 6.0 μmol/L in the inner estuary and 9.4 μmol/L in the outer estuary (Figure 8b). In addition to the DOM quantity, we also analyzed the DOM characteristics inside and outside the sediment traps (Figures 8c–8h). Overall, the observed patterns were very similar for the inner and outer estuary. There was a decrease in δ^{13}C-DOC values by approximately 1‰ (Figure 8c). Additionally, HIX and DOC-normalized humic-like fluorescence decreased during the trap deployments (Figures 8d and 8f). There was an increase in DOC-normalized protein-like fluorescence (Figure 8e) and also in DOC-normalized protein-like fluorescence components C8 and C9. It should be noted that observed values of C9 were virtually 0 in the ambient water, indicating that this component was produced inside the sediment trap. Changes in all PARAFAC components and BIX are shown in Figure S2. Overall, changes in the quantity and the quality of the DOM pools after the 24-hr in situ incubation in the sediment traps were very similar in both inner and outer estuary, despite differences in salinity and DOC concentration.
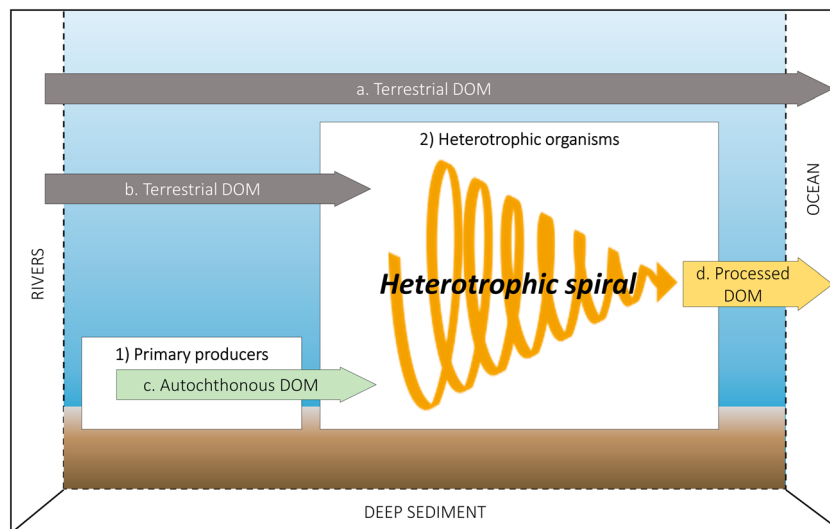
Figure 9. Proposed schematic of the conceptual *heterotrophic spiral* showing the DOM pathways in coastal environments. Dashed box indicates the system boundaries of the coastal environment. Four different DOM pools are identified: (a) terrestrial DOM that passes through the system unaltered (conservative mixing), (b) terrestrial DOM that is intercepted by the heterotrophic spiral, (c) autochthonous DOM originating from the primary production within the system, and (d) DOM processed in the heterotrophic spiral leaving the system. The two major biological groups are (1) aquatic primary producers (e.g., phytoplankton, macrophytes, and microphytobenthos) within the system producing autochthonous DOM and (2) heterotrophic organisms (such as bacteria, protozooplankton, zooplankton, and macrofauna) consuming, transforming, and producing DOM within the system. DOM = dissolved organic matter.

4. Discussion

Anthropogenic nutrient inputs are causing increased organic matter production in coastal areas globally (Cloern, 2001). Results from this study suggest that a considerable proportion of this autochthonous organic matter rapidly becomes processed on its way to the open sea. In the process, a major proportion of the fresh autochthonous organic matter is transformed into more recalcitrant, semilabile, or even semirefractory DOM (following nomenclature by Hansell (2013). This process is analogous to the *spiraling* concept, which in lotic systems has been used to conceptualize turnover of carbon and nutrients along spatial gradients. In this chain of biogeochemical processes, carbon and nutrients are assimilated from the water column into biomass, temporarily retained, and remineralized back into the water column (Ensign & Doyle, 2006; Newbold et al., 1982). This spiral, where nutrients and organic carbon are being utilized by heterotrophic organisms, gradually reduces the bioavailability of the remaining pool (Figure 9). The estuary in this study can be considered as a model system, because the low freshwater inputs and the consequent long residence times allow extensive processing of nutrients and carbon. Also, relatively high inputs of inorganic nutrients and low inputs of terrestrial organic carbon reduce the masking of autochthonous organic carbon by allochthonous inputs. As Roskilde Fjord is not light limited, high nutrient loads can effectively fuel benthic and pelagic primary production, contrasting with systems with high freshwater inflow, which are usually associated with high suspended particle and CDOM inputs and short residence times. Thus, in those systems there is insufficient processing time to alter the organic carbon pools markedly, making it difficult to trace changes in the DOM pool by the typical analytical approaches. While these results only stem from one estuary, we assume that the spiraling concept described here is ubiquitous in eutrophic coastal areas. The time scales of process rates relative to freshwater residence time will, however, determine whether a given system follows conservative or nonconservative mixing.

In temperate coastal systems, DIN is potentially limiting primary production in late spring and summer (Staehr et al., 2017). Denitrification rates are also highest during summer months, further amplifying nitrogen depletion (Pina-Ochoa & Alvarez-Cobelas, 2006). We observed this seasonal pattern in the marine stations, whereas the notable increase in DIP at the inner station during late summer suggests sediment release of DIP (Riemann et al., 2016). External inputs during that time are low, and the high temperatures enhance microbial processing in the sediments (Aller & Benninger, 1981; Søndergaard et al., 2013). The observed

large production of DIP and large consumption of DIN in the inner estuary underlines the differences in the cycling of these two elements in coastal systems (Asmala et al., 2016; Knudsen-Leerbeck et al., 2017). Also, a major pathway for nitrogen is the transformation of inorganic to organic forms, reducing nitrogen bioavailability significantly (Jørgensen et al., 2014). In our study, this transformation of inorganic nitrogen to recalcitrant DON was evident in both basin-scale observations and in the 24-hr in situ bioassays.

The spiraling process was also observed as change in the DOM quality characteristics, which are known to exhibit seasonal patterns in temperate coastal waters (Keith et al., 2002; Markager et al., 2011). Typically, coastal DOM in spring has a more pronounced terrestrial signal because of the higher freshwater inputs from the catchment during winter and lower level of processing associated with lower temperatures. In contrast, in autumn DOM has less terrestrial signal due to lower freshwater discharge and higher autochthonous DOM production. Due to longer residence time, this DOM has been processed further within the system, resulting in less bioavailable DOM compared to the *fresh* DOM from the freshwater system in spring or autochthonous DOM in summer (Wiegner & Seitzinger, 2004; Stedmon et al., 2006). Also, photochemical degradation transforms the DOM pool of the surface waters but in general results in increased bioavailability of DOM photoproducts (Moran & Zepp, 1997). Inherent photochemical reactivity of DOM in the Baltic Sea does not vary seasonally, but pronounced seasonality in solar radiation and changes in bacterial affinity to photoproducts may lead to high utilization of DOM altered by photochemical reactions during summer (Aarnos et al., 2012). The seasonal variation in the bulk DOM was confirmed by the seasonal sampling in the study. Overall, the decrease in annual variability when moving from freshwater to higher salinities indicates that exchange with the open sea was buffering seasonal changes.

Seasonal dynamics of DOM in freshwater streams and rivers is dependent on the climatic and weather-related drivers and also on the catchment land use and characteristics (Stedmon et al., 2006). Effectively, freshwater dynamics are driven by precipitation, groundwater infiltration, and other catchment-related processes with the strongest terrestrial signal in spring. In eutrophic systems like Roskilde Fjord, where internal production of organic matter by far exceeds external inputs, the annual cycle may be different from the typical estuarine or coastal patterns. Recently, it has also been shown that remineralization of DON provided almost half of the bioavailable nitrogen in Roskilde Fjord and together with sediment is the dominating source of bioavailable nitrogen for production during the productive season when external inputs are not enough to fulfill the nutrient demand (Knudsen-Leerbeck et al., 2017). This emphasizes the importance of DOM for nutrient cycling and in general the dynamic nature of DOM in estuaries.

We were able to distinguish the different fingerprints of streamwater, inner estuary, and outer estuary DOM. From these fingerprints, we observed an inverse pattern in the annual cycle of DOC concentration between freshwater and marine stations, and the pattern observed in the marine system was driven by the autochthonous production of organic matter, peaking in late summer. The direct influence of the freshly produced organic matter was apparent in the dynamics of the protein-like FDOM and BIX, which are both linked to autochthonous production (Huguet et al., 2009; Murphy et al., 2008). The summer maxima of these characteristics in the marine stations indicate high autochthonous influence in this period.

Eutrophic coastal systems with relatively high nutrient and low organic matter inputs can be seen as reactors, where nutrients are catalyzing the production of autochthonous organic matter within the system (Markager et al., 2011). Our study corroborates this view and provides insight about the characteristics of the organic matter being produced and transformed in this reactor. We observed consistent changes in the DOM pool toward increasing UV absorption, smaller average molecular size, and increasing protein-to-humic-like fluorescence properties in the DOM pool. In other words, the accumulating DOM is unexpectedly protein-like (*autochthonous*), not humic-like (*allochthonous*). These accumulating organic compounds are likely amino acids and amino sugars derived from bacterial cell growth and decline (Kawasaki & Benner, 2006; Koch et al., 2014). A number of amino acids are detectable from oceanic refractory DOM pool, resisting biological decay for prolonged periods (Kaiser & Benner, 2008; McCarthy et al., 1998). An alternative source for autochthonous organic matter in the coastal zone would be sediments, but the major fraction of the DOM released by benthic mineralization is humic-like (Luek et al., 2017), which was observed decreasing in our study. Also, photooxidation of DOM would lead to smaller molecules and decreased humic-like fluorescence signal, as the process is selective to humic-like compounds in the DOM pool (Hansen et al., 2016; Moran et al., 2000; Moran & Zepp, 1997), but would also decrease the bulk amount of DOM by degrading DOC to carbon

monoxide and dissolved inorganic carbon (Miller & Zepp, 1995). As our observations show net increase of DOC in the inner estuary, the effect of photodegradation to bulk considerations can be seen smaller than the autochthonous production. However, during periods of high solar radiation, photodegradation likely transforms the DOM pool to some extent, but these changes are masked by the high autochthonous production of organic matter and its biological processing in the system (Moran et al., 2000). Biological processing of organic matter results in changes in its isotopic composition, as lighter isotopes of, for example, carbon and nitrogen are utilized preferentially over heavier ones (Fry & Sherr, 1989). Consequently, the isotopic values of the remaining organic matter pool becomes gradually heavier. From our sediment trap data, we observed that δ^{13}C-DOC values were lower after the 24-hr deployments, which indicates rapid biological fractionation of the autochthonous DOM, as heterotrophic degradation typically lowers the δ^{13}C values of the remaining DOC pool (Hullar et al., 1996). Also, this indicates that organic matter is being transformed from particulate to dissolved pool as a result of heterotrophic degradation, as supported by the increase in DOC concentration during the deployments. This suggests that heterotrophic transformations of organic matter from POM to DOM occurs over relatively short time scales of less than 24 hr. It should be noted that sediment traps artificially concentrate planktonic and detrital material, which might lead to elevated process rates compared to undisturbed system. However, the changes in DOM pool observed in the sediment traps are strikingly similar to the large-scale changes observed in the inner estuary. The changes in isotopic composition and other DOM variables are rather consistent in both inner and outer parts of the estuary, and this observation coupled to changes in other DOM characteristics indicate that the same biological transformation processes occur throughout the estuary.

Our results deviate from findings from studies carried out in aquatic systems that are not eutrophic. Typically, inorganic nutrient limitation leads to preferred utilization of N-rich DOM, as indicated by low DOC:DON ratio or protein-like FDOM (Asmala et al., 2013; Fellman et al., 2008). Also, in noneutrophic systems humic-like FDOM is accumulated as a result of bacterial processing of phytoplankton exudates (Kinsey et al., 2017). From this follows that in environments where nitrogen is abundant, C:N ratio or protein-like properties (indicative of N-rich organic molecules) are not accurate predictors of DOM bioavailability. This is likely also the case with phosphate and organic phosphorus, but our data are too scarce to corroborate that. In other words, in coastal systems with high nutrient inputs the DOM recalcitrance is driven by something else than the traditional indices based on its inherent properties, such as C:N:P stoichiometry, but also on the environmental conditions (Marín-Spiotta et al., 2014).

In conclusion, we documented significant changes in DOM quantity and characteristics along a freshwater to marine gradient as a result of physical mixing and biochemical processes in a eutrophic coastal system with high nutrient inputs and a long freshwater residence time. Through combining multiple characterization methods, we quantified the rapid transformation of phytoplankton-derived autochthonous POM and DOM into a pool of biologically recalcitrant DOM exported to the open sea. This DOM pool is characterized by small molecule size and protein-like fluorescent properties. Our findings demonstrate that the potentially high initial bioavailability of the autochthonous organic matter was rapidly lost through the cycling in the heterotrophic spiral.

References

Aarnos, H., Ylöstalo, P., & Vähätalo, A. V. (2012). Seasonal phototransformation of dissolved organic matter to ammonium, dissolved inorganic carbon, and labile substrates supporting bacterial biomass across the Baltic Sea. *Journal of Geophysical Research*, *117*, G01004. https://doi.org/10.1029/2010JG001633

Abril, G., Nogueira, M., Etcheber, H., Cabeçadas, G., Lemaire, E., & Brogueira, M. (2002). Behaviour of organic carbon in nine contrasting European estuaries. *Estuarine, Coastal and Shelf Science*, *54*(2), 241–262. https://doi.org/10.1006/ecss.2001.0844

Aller, R., & Benninger, L. (1981). Spatial and temporal patterns of dissolved ammonium, manganese and silica fluxes from bottom sediments of Long Island Sound, USA. *Journal of Marine Research*, *39*, 295–314.

Amon, R. M., & Benner, R. (1996). Bacterial utilization of different size classes of dissolved organic matter. *Limnology and Oceanography*, *41*(1), 41–51. https://doi.org/10.4319/lo.1996.41.1.0041

Asmala, E., Autio, R., Kaartokallio, H., Pitkänen, L., Stedmon, C., & Thomas, D. N. (2013). Bioavailability of riverine dissolved organic matter in three Baltic Sea estuaries and the effect of catchment land use. *Biogeosciences*, *10*(11), 6969–6986.

Asmala, E., Bowers, D. G., Autio, R., Kaartokallio, H., & Thomas, D. N. (2014). Qualitative changes of riverine dissolved organic matter at low salinities due to flocculation. *Journal of Geophysical Research: Biogeosciences*, *119*, 1919–1933. https://doi.org/10.1002/2014JG002722

Asmala, E., Haraguchi, L., Jakobsen, H. H., Massicotte, P., & Carstensen, J. (2018). Nutrient availability as major driver of phytoplankton-derived dissolved organic matter transformation in coastal environment. *Biogeochemistry*, *137*(1–2), 93–104. https://doi.org/10.1007/s10533-017-0403-0

Asmala, E., Kaartokallio, H., Carstensen, J., & Thomas, D. N. (2016). Variation in riverine inputs affect dissolved organic matter characteristics throughout the estuarine gradient. *Frontiers in Marine Science*, *2*, 125.

Bertilsson, S., & Jones, J. (2003). Supply of dissolved organic matter to aquatic ecosystems: Autochthonous sources. In *Aquatic ecosystems: interactivity of dissolved organic matter* (pp. 3–24). Academic Press. Retrieved from https://www.sciencedirect.com/book/9780122563713/aquatic-ecosystems, https://doi.org/10.1016/B978-012256371-3/50002-0

Boesch, D. F. (2002). Challenges and opportunities for science in reducing nutrient over-enrichment of coastal ecosystems. *Estuaries and Coasts*, *25*(4), 886–900. https://doi.org/10.1007/BF02804914

Bowers, D., & Brett, H. (2008). The relationship between CDOM and salinity in estuaries: An analytical and graphical solution. *Journal of Marine Systems*, *73*(1–2), 1–7. https://doi.org/10.1016/j.jmarsys.2007.07.001

Bowers, D., Evans, D., Thomas, D., Ellis, K., & Williams, P. L. B. (2004). Interpreting the colour of an estuary. *Estuarine, Coastal and Shelf Science*, *59*(1), 13–20. https://doi.org/10.1016/j.ecss.2003.06.001

Chin, Y., Aiken, G., & O'Loughlin, E. (1994). Molecular weight, polydispersity, and spectroscopic properties of aquatic humic substances. *Environmental Science & Technology*, *28*(11), 1853–1858. https://doi.org/10.1021/es00060a015

Cloern, J. E. (2001). Our evolving conceptual model of the coastal eutrophication problem. *Marine Ecology Progress Series*, *210*, 223–253. https://doi.org/10.3354/meps210223

Cloern, J. E., Foster, S., & Kleckner, A. (2014). Phytoplankton primary production in the world's estuarine-coastal ecosystems. *Biogeosciences*, *11*(9), 2477–2501. https://doi.org/10.5194/bg-11-2477-2014

Coble, P. G. (1996). Characterization of marine and terrestrial DOM in seawater using excitation-emission matrix spectroscopy. *Marine Chemistry*, *51*(4), 325–346. https://doi.org/10.1016/0304-4203(95)00062-3

Cole, J. J., Prairie, Y. T., Caraco, N. F., McDowell, W. H., Tranvik, L. J., Striegl, R. G., et al. (2007). Plumbing the global carbon cycle: Integrating inland waters into the terrestrial carbon budget. *Ecosystems*, *10*(1), 172–185. https://doi.org/10.1007/s10021-006-9013-8

Conley, D. J., Markager, S., Andersen, J., Ellermann, T., & Svendsen, L. M. (2002). Coastal eutrophication and the Danish national aquatic monitoring and assessment program. *Estuaries and Coasts*, *25*(4), 848–861. https://doi.org/10.1007/BF02804910

Conley, D. J., Paerl, H. W., Howarth, R. W., Boesch, D. F., Seitzinger, S. P., Havens, K. E., et al. (2009). Controlling eutrophication: Nitrogen and phosphorus. *Science*, *323*(5917), 1014–1015. https://doi.org/10.1126/science.1167755

Ensign, S. H., & Doyle, M. W. (2006). Nutrient spiraling in streams and river networks. *Journal of Geophysical Research*, *111*, G04009. https://doi.org/10.1029/2005JG000114

Fellman, J. B., D'Amore, D. V., Hood, E., & Boone, R. D. (2008). Fluorescence characteristics and biodegradability of dissolved organic matter in forest and wetland soils from coastal temperate watersheds in southeast Alaska. *Biogeochemistry*, *88*(2), 169–184. https://doi.org/10.1007/s10533-008-9203-x

Fry, B., & Sherr, E. B. (1989). δ^{13}C measurements as indicators of carbon flow in marine and freshwater ecosystems. In P. Rundel, J. R. Ehleringer, & K. A. Nagy (Eds.), *Stable isotopes in ecological research*, (pp. 196–229). New York: Springer-Verlag. https://doi.org/10.1007/978-1-4612-3498-2

Guo, W., Stedmon, C. A., Han, Y., Wu, F., Yu, X., & Hu, M. (2007). The conservative and non-conservative behavior of chromophoric dissolved organic matter in Chinese estuarine waters. *Marine Chemistry*, *107*(3), 357–366. https://doi.org/10.1016/j.marchem.2007.03.006

Hansell, D. A. (2013). Recalcitrant dissolved organic carbon fractions. *Annual Review of Marine Science*, *5*, 421–445. https://doi.org/10.1146/annurev-marine-120710-100757

Hansell, D. A., Carlson, C. A., Repeta, D. J., & Schlitzer, R. (2009). Dissolved organic matter in the ocean: A controversy stimulates new insights. *Oceanography*, *22*(4), 202–211. https://doi.org/10.5670/oceanog.2009.109

Hansen, A. M., Kraus, T. E., Pellerin, B. A., Fleck, J. A., Downing, B. D., & Bergamaschi, B. A. (2016). Optical properties of dissolved organic matter (DOM): Effects of biological and photolytic degradation. *Limnology and Oceanography*, *61*(3), 1015–1032. https://doi.org/10.1002/lno.10270

Hansen, H. P., & Koroleff, F. (1999). Determination of nutrients. In K. Grasshoff, K. Kremling, & M. Ehrhardt (Eds.), *Methods of seawater analysis* (pp. 159–228). Weinheim, Germany: Wiley-VCH Verlag.

Hartigan, J. A., & Wong, M. A. (1979). Algorithm AS 136: A *k*-means clustering algorithm. *Journal of the Royal Statistical Society: Series C: Applied Statistics*, *28*, 100–108.

Hastie, T., & Tibshirani, R. (1990). *Generalized additive models*. London: Chapman and Hall.

Hopkinson, C. S., Buffam, I., Hobbie, J., Vallino, J., Perdue, M., Eversmeyer, B., et al. (1998). Terrestrial inputs of organic matter to coastal ecosystems: An intercomparison of chemical characteristics and bioavailability. *Biogeochemistry*, *43*(3), 211–234. https://doi.org/10.1023/A:1006016030299

Huguet, A., Vacher, L., Relexans, S., Saubusse, S., Froidefond, J., & Parlanti, E. (2009). Properties of fluorescent dissolved organic matter in the Gironde estuary. *Organic Geochemistry*, *40*(6), 706–719. https://doi.org/10.1016/j.orggeochem.2009.03.002

Hullar, M., Fry, B., Peterson, B. J., & Wright, R. T. (1996). Microbial utilization of estuarine dissolved organic carbon: A stable isotope tracer approach tested by mass balance. *Applied and Environmental Microbiology*, *62*(7), 2489–2493.

Jiao, N., Herndl, G. J., Hansell, D. A., Benner, R., Kattner, G., Wilhelm, S. W., et al. (2010). Microbial production of recalcitrant dissolved organic matter: Long-term carbon storage in the global ocean. *Nature Reviews. Microbiology*, *8*, 593.

Jørgensen, L., Markager, S., & Maar, M. (2014). On the importance of quantifying bioavailable nitrogen instead of total nitrogen. *Biogeochemistry*, *117*(2-3), 455–472. https://doi.org/10.1007/s10533-013-9890-9

Kaiser, K., & Benner, R. (2008). Major bacterial contribution to the ocean reservoir of detrital organic carbon and nitrogen. *Limnology and Oceanography*, *53*(1), 99–112. https://doi.org/10.4319/lo.2008.53.1.0099

Kamp-Nielsen, L. (1992). Benthic-pelagic coupling of nutrient metabolism along an estuarine eutrophication gradient. *Hydrobiologia*, *235*(1), 457–470.

Kawasaki, N., & Benner, R. (2006). Bacterial release of dissolved organic matter during cell growth and decline: Molecular origin and composition. *Limnology and Oceanography*, *51*(5), 2170–2180. https://doi.org/10.4319/lo.2006.51.5.2170

Keith, D., Yoder, J., & Freeman, S. (2002). Spatial and temporal distribution of coloured dissolved organic matter (CDOM) in Narragansett Bay, Rhode Island: Implications for phytoplankton in coastal waters. *Estuarine, Coastal and Shelf Science*, *55*(5), 705–717. https://doi.org/10.1006/ecss.2001.0922

Kinsey, J. D. K., Corradino, G., Ziervogel, K., Schnetzer, A., & Osburn, C. L. (2017). Formation of chromophoric dissolved organic matter by bacterial degradation of phytoplankton-derived aggregates. *Frontiers in Marine Science*, *4*, 430.

Knudsen-Leerbeck, H., Mantikci, M., Bentzon-Tilia, M., Traving, S. J., Riemann, L., Hansen, J. L., & Markager, S. (2017). Seasonal dynamics and bioavailability of dissolved organic matter in two contrasting temperate estuaries. *Biogeochemistry*, *134*(1–2), 217–236. https://doi.org/10.1007/s10533-017-0357-2

Koch, B., Kattner, G., Witt, M., & Passow, U. (2014). Molecular insights into the microbial formation of marine dissolved organic matter: Recalcitrant or labile? *Biogeosciences*, *11*(15), 4173–4190. https://doi.org/10.5194/bg-11-4173-2014

Luek, J. L., Thompson, K. E., Larsen, R. K., Heyes, A., & Gonsior, M. (2017). Sulfate reduction in sediments produces high levels of chromophoric dissolved organic matter. *Scientific Reports*, *7*, 8829.

Mantoura, R., & Woodward, E. (1983). Conservative behaviour of riverine dissolved organic carbon in the Severn estuary: Chemical and geochemical implications. *Geochimica et Cosmochimica Acta*, *47*(7), 1293–1309. https://doi.org/10.1016/0016-7037(83)90069-8

Marín-Spiotta, E., Gruley, K., Crawford, J., Atkinson, E., Miesel, J., Greene, S., et al. (2014). Paradigm shifts in soil organic matter research affect interpretations of aquatic carbon cycling: Transcending disciplinary and ecosystem boundaries. *Biogeochemistry*, *117*(2-3), 279–297. https://doi.org/10.1007/s10533-013-9949-7

Markager, S., Stedmon, C. A., & Søndergaard, M. (2011). Seasonal dynamics and conservative mixing of dissolved organic matter in the temperate eutrophic estuary Horsens Fjord. *Estuarine, Coastal and Shelf Science*, *92*(3), 376–388. https://doi.org/10.1016/j.ecss.2011.01.014

Massicotte, P. (2018). eemR: Tools for Pre-Processing Emission-Excitation-Matrix (EEM) Fluorescence Data. R package version 0.1.5.9000. Retrieved from https://github.com/PMassicotte/eemR

McCarthy, M. D., Hedges, J. I., & Benner, R. (1998). Major bacterial contribution to marine dissolved organic nitrogen. *Science*, *281*(5374), 231–234. https://doi.org/10.1126/science.281.5374.231

Miller, W. L., & Zepp, R. G. (1995). Photochemical production of dissolved inorganic carbon from terrestrial organic matter: Significance to the oceanic organic carbon cycle. *Geophysical Research Letters*, *22*(4), 417–420.

Moran, M. A., Sheldon, W. M., & Zepp, R. G. (2000). Carbon loss and optical property changes during long-term photochemical and biological degradation of estuarine dissolved organic matter. *Limnology and Oceanography*, *45*(6), 1254–1264. https://doi.org/10.4319/lo.2000.45.6.1254

Moran, M. A., & Zepp, R. G. (1997). Role of photoreactions in the formation of biologically labile compounds from dissolved organic matter. *Limnology and Oceanography*, *42*(6), 1307–1316. https://doi.org/10.4319/lo.1997.42.6.1307

Murphy, K. R., Butler, K. D., Spencer, R. G., Stedmon, C. A., Boehme, J. R., & Aiken, G. R. (2010). Measurement of dissolved organic matter fluorescence in aquatic environments: An interlaboratory comparison. *Environmental Science & Technology*, *44*(24), 9405–9412. https://doi.org/10.1021/es102362t

Murphy, K. R., Stedmon, C. A., Graeber, D., & Bro, R. (2013). Fluorescence spectroscopy and multi-way techniques. PARAFAC. *Analytical Methods*, *5*(23), 6557–6566. https://doi.org/10.1039/c3ay41160e

Murphy, K. R., Stedmon, C. A., Waite, T. D., & Ruiz, G. M. (2008). Distinguishing between terrestrial and autochthonous organic matter sources in marine environments using fluorescence spectroscopy. *Marine Chemistry*, *108*(1-2), 40–58. https://doi.org/10.1016/j.marchem.2007.10.003

Myklestad, S. M. (1995). Release of extracellular products by phytoplankton with special emphasis on polysaccharides. *Science of the Total Environment*, *165*(1-3), 155–164. https://doi.org/10.1016/0048-9697(95)04549-G

Nagata, T., Fukuda, H., Fukuda, R., & Koike, I. (2000). Bacterioplankton distribution and production in deep Pacific waters: Large–scale geographic variations and possible coupling with sinking particle fluxes. *Limnology and Oceanography*, *45*(2), 426–435. https://doi.org/10.4319/lo.2000.45.2.0426

Newbold, J., Mulholland, P., Elwood, J., & O'Neill, R. (1982). Organic carbon spiralling in stream ecosystems. *Oikos*, *38*(3), 266–272.

Officer, C. B. (1979). Discussion of the behaviour of nonconservative dissolved constituents in estuaries. *Estuarine and Coastal Marine Science*, *9*(1), 91–94. https://doi.org/10.1016/0302-3524(79)90009-4

Pedersen, T. M., Sand-Jensen, K., Markager, S., & Nielsen, S. L. (2014). Optical changes in a eutrophic estuary during reduced nutrient loadings. *Estuaries and Coasts*, *37*(4), 880–892. https://doi.org/10.1007/s12237-013-9732-y

Pina-Ochoa, E., & Alvarez-Cobelas, M. (2006). Denitrification in aquatic environments: A cross-system analysis. *Biogeochemistry*, *81*(1), 111–130. https://doi.org/10.1007/s10533-006-9033-7

Riemann, B., Carstensen, J., Dahl, K., Fossing, H., Hansen, J. W., Jakobsen, H. H., et al. (2016). Recovery of Danish coastal ecosystems after reductions in nutrient loading: A holistic ecosystem approach. *Estuaries and Coasts*, *39*(1), 82–97. https://doi.org/10.1007/s12237-015-9980-0

Rochelle-Newall, E., & Fisher, T. (2002). Production of chromophoric dissolved organic matter fluorescence in marine and estuarine environments: An investigation into the role of phytoplankton. *Marine Chemistry*, *77*(1), 7–21. https://doi.org/10.1016/S0304-4203(01)00072-X

Søndergaard, M., Bjerring, R., & Jeppesen, E. (2013). Persistent internal phosphorus loading during summer in shallow eutrophic lakes. *Hydrobiologia*, *710*(1), 95–107. https://doi.org/10.1007/s10750-012-1091-3

Søndergaard, M., & Middelboe, M. (1995). A cross-system analysis of labile dissolved organic carbon. *Marine Ecology Progress Series*, *118*, 283–294.

Spencer, R. G., Ahad, J. M., Baker, A., Cowie, G. L., Ganeshram, R., Upstill-Goddard, R. C., & Uher, G. (2007). The estuarine mixing behaviour of peatland derived dissolved organic carbon and its relationship to chromophoric dissolved organic matter in two North Sea estuaries (UK). *Estuarine, Coastal and Shelf Science*, *74*(1-2), 131–144. https://doi.org/10.1016/j.ecss.2007.03.032

Staehr, P. A., Asmala, E., Carstensen, J., Krause-Jensen, D., & Reader, H. (2018). Ecosystem metabolism of benthic and pelagic zones of a shallow productive estuary: Spatio-temporal variability. *Marine Ecology Progress Series*, *601*, 15–32. https://doi.org/10.3354/meps12697

Staehr, P. A., Testa, J., & Carstensen, J. (2017). Decadal changes in water quality and net productivity of a shallow Danish estuary following significant nutrient reductions. *Estuaries and Coasts*, *40*(1), 63–79. https://doi.org/10.1007/s12237-016-0117-x

Stedmon, C. A., Markager, S., & Bro, R. (2003). Tracing dissolved organic matter in aquatic environments using a new approach to fluorescence spectroscopy. *Marine Chemistry*, *82*(3-4), 239–254. https://doi.org/10.1016/S0304-4203(03)00072-0

Stedmon, C. A., Markager, S., Søndergaard, M., Vang, T., Laubel, A., Borch, N. H., & Windelin, A. (2006). Dissolved organic matter (DOM) export to a temperate estuary: Seasonal variations and implications of land use. *Estuaries and Coasts*, *29*(3), 388–400. https://doi.org/10.1007/BF02784988

Uher, G., Hughes, C., Henry, G., & Upstill-Goddard, R. C. (2001). Non-conservative mixing behavior of colored dissolved organic matter in a humic-rich, turbid estuary. *Geophysical Research Letters*, *28*(17), 3309–3312. https://doi.org/10.1029/2000GL012509

Vähätalo, A. V., Aarnos, H., & Mäntyniemi, S. (2010). Biodegradability continuum and biodegradation kinetics of natural organic matter described by the beta distribution. *Biogeochemistry*, *100*(1-3), 227–240. https://doi.org/10.1007/s10533-010-9419-4

Vartiainen, T., Liimatainen, A., & Kauranen, P. (1987). The use of TSK size exclusion columns in determination of the quality and quantity of humus in raw waters and drinking waters. *Science of the Total Environment*, *62*, 75–84. https://doi.org/10.1016/0048-9697(87)90484-0

Wiegner, T. N., & Seitzinger, S. P. (2004). Seasonal bioavailability of dissolved organic carbon and nitrogen from pristine and polluted freshwater wetlands. *Limnology and Oceanography*, *49*(5), 1703–1712. https://doi.org/10.4319/lo.2004.49.5.1703

Wood, S. N. (2011). Fast stable restricted maximum likelihood and marginal likelihood estimation of semiparametric generalized linear models. *Journal of the Royal Statistical Society, Series B: Statistical Methodology*, *73*(1), 3–36. https://doi.org/10.1111/j.1467-9868.2010.00749.x

Zsolnay, A., Baigar, E., Jimenez, M., Steinweg, B., & Saccomandi, F. (1999). Differentiating with fluorescence spectroscopy the sources of dissolved organic matter in soils subjected to drying. *Chemosphere*, *38*(1), 45–50. https://doi.org/10.1016/S0045-6535(98)00166-0